Int. J. Electrochem. Sci., 4 **(2009)** 60 - 76

International Journal of ELECTROCHEMICAL SCIENCE
www.electrochemsci.org

Study of Electrical Resistance on the Surface of Nafion 115® Membrane Used as Electrolyte in PEMFC Technology Part II: Surface Response Methodology

C. Moisés Bautista-Rodríguez[1,], Araceli Rosas-Paleta[2], J. Antonio Rivera-Márquez[1], Omar Solorza-Feria[3]*

[1] Alter Energías Grupo. Tepetitlán No. 63, Col. Lomas del Sur, CP 72470 Puebla, Pue. México
[2] BUAP. Facultad de Ingeniería Química. Av. San Claudio y 18 Sur - CU-, 72590 Puebla, Pue. México
[3] Cinvestav-IPN. Depto de Química. Av. IPN 2508, Col. San Pedro Zacatenco. C.P. 07360 México DF, México
[*] Actual address: UHDE de México S.A. Av. Paseo de las Palmas 405. CP 11000 Lomas de Chapultepec, DF. México, E-mail: celso.bautista@thyssenkrupp.com

Received: 17 Septmeber 2008 / *Accepted:* 6 December 2008 / *Published:* 20 December 2008

The membrane Nafion® is commonly used as a polymer electrolyte fuel cell technology, particulary for the proton exchange membrane fuel cell (PEMFC) and Direct Methanol Fuel Cell (DMFC). Ionic conductivity, mechanical and chemical resistances are the main characteristics for obtaining a good efficiency in the PEMFC and DMFC performance. The conductivity in the membrane Nafion® in combination with their morphological characteristics allows the development of different phenomena as kinetics and transports (mass, electrons and freight) during operation of the PEMFC. The phenomena mentioned are performed in the interface electrode-electrolyte, where is located a triple contact area; electrode-catalyst-electrolyte. The present study is focused on the probably Nafion membrane effect when electrons are traversing the membrane to the active sites on the electrodes, this effect may be the principal cause of increases in the ohmic losses. This paper presents the results of analysis of response surface applied on the records of superficial measure electrical resistance on both sides of membrane Nafion 115 ®. A first analysis has been applied on activated Nafion 115 and a second analysis on a not activated membrane. The results show heterogeneity on the membrane surface for electrical resistance property at both sides and both for the two membranes, where the average value of electrical resistance surface is ten times lower in the activated membrane. The surface responses graphics present different levels in electrical resistance propriety involving the presence of maximum and minimum values, these features may have a significant impact on the PEMFC functionality.

Keywords: Nafion, PEMFC performance, Conductance, Electrical Resistance

1. INTRODUCTION

Actually, the main Interest in the Nafion stems from the properties of this membrane which involved about functionality in fuel cell technologies, promising technologies in power generation. Particularly, the proton exchange membrane fuel cell (PEMFC) is regarded as an electrochemical device that converts chemical energy from chemical compounds (hydrogen and oxygen) into electrical energy producing water as a byproduct. This device operates at temperatures below 120 ° C with pressures of operating between 1 and 5 bar and efficiencies by around 65%, being considered in stationary and mobile devices, other advantages of the PEMFC are; easy refueling, long time of life functional producing energy, flexibility between power (watts) and ability, that is; mono-cells applied in low-voltage systems and stacks used in high voltage systems. Nowadays, many studies are focused on the implementation of the PEMFC in transportation systems from cars or buses, the latter being used in tourism services in major cities around the world. In stationary services the PEMFC generators are used as domestic, public and private services [1-14].

A mono-cell PEMFC is normally constituted by four core elements: 1) porous electrodes loaded by catalysts based on noble metals (Platinum, Ruthenium, etc.) or alloys; 2) semi-solid electrolyte (Nafion membrane); 3) polar plates with channels as gas fuels distributors (metallic or graphite) and 4) external electrical circuit where driving the flow of electrons generated in the anode electrode towards the cathodic electrode. It is in the cathodic electrode where the overall reaction is completed to produce water [7-11]. The PEMFC functionality is typically characterized by a current - potential curve as presented in Figure 1, where four areas are classified operating according to the tension exerted on the fuel cell. The first area is characterized by a loss in tension generated by Redox reactions irreversibility developing on the active layer of the electrodes in the fuel cell, the second area is characterized by activation losses on electro - catalytic sites in the diffusive electrodes. The interest of this study is focused on the third area, this is characterized by ohmic losses in the electrode - electrolyte interface and this area includes the conductivity effects (ionic, change and electronic) of Nafion membrane on the PEMFC performance [10-12]. The fourth area is characterized by loss of dissemination in the feeding of reactive gases caused by various phenomena of mass transport (reagents and products) in the porous electrodes.

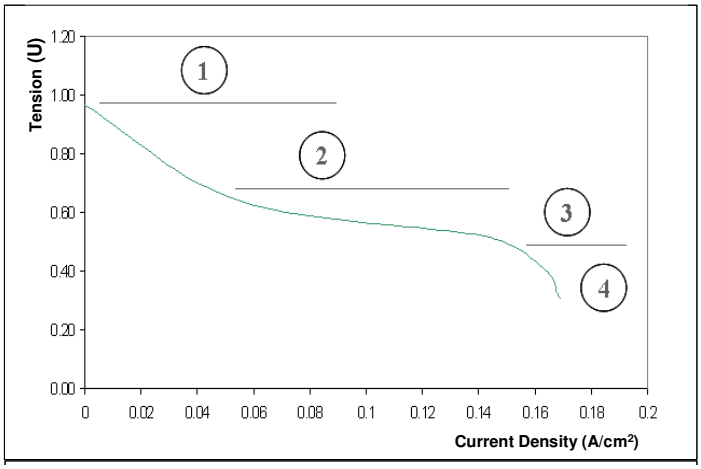

Figure 1. Performance curve and characterization zones for a PEM Fuel Cell functionality.

In a PEMFC operating, hydrogen current is flowing by the channels distributors (mass transport) in the anodic polar plate (metallic or graphite) at the diffusion layer on the anode electrode. Hydrogen current is conduced by micro-pores (mass transport) at the active layer (triple contact area), site where the hydrogen reacts to generate protons (kinetics), which are conducted (ionic transport) by the electrolyte (Nafion membrane) at the active layer of the cathodic electrode, consequently, the value of the ionic conductivity (Proton) in the polymer electrolyte is essential for the PEMFC functionality. Moreover, the electrons migrate in the opposite direction toward the polar plates (electronic transport), due to non-electronic-conductive properties in the film and Nafion membrane, generating a ohmic losses represented in zone 3 on the performance curve (Figure 1). Figure 2 outlines the processes developed in the anodic electrode. Moreover, the overall reaction on the cathodic electrode as follows: electronic transport is done in reverse, i.e.; electrons generated in the anode are collected by an external circuit connected to the cathodic polar plate, here the electros are distributed on the surface of the active layer in the cathodic electrode through the diffusion layer. The oxygen flow is transported in the same direction at the active sites and protons arrive by the electrolyte to the active layer then the three elements reacts producing water. Electrons must overcome the electrical resistance of the Nafion film and membrane to reach the active sites (triple contact area) and perform in conjunction with the overall reaction (water). It is important to mention that some quantity of electrical energy is converted in thermal energy by electrons to overcome the electrical resistance in film and Nafion membrane, and then it's expected to result in a ohmic losses on the PEMFC performance. Figure 3 presents the above processes in the triple contact area on the cathodic electrode. Specifically, the properties of Nafion membrane involved in the PEMFC functionality are: proton conductivity, water management, stability in their hydration to the operating temperatures of the PEMFC, drag electro-osmotic, chemical stability, mechanical and thermal present at the Nafion membrane [3,4,13-14]. Moreover, several authors have published the values for ionic conductivity in the Nafion membrane [15-20], reporting that overall conductivity in the membrane is a function of the volume of water contained (relative humidity) in the membrane. The values reported are the order of 10^{-2} S cm^{-1} to 100% relative humidity. Particularly, Fontanella and co. [20] has reported electrical conductivity measurements obtained by impedance spectroscopy, their values have been measured between 0 and 0.10 S cm-1 for the membrane N117 and N120 with water content between 3 and 30 wt% respectively.

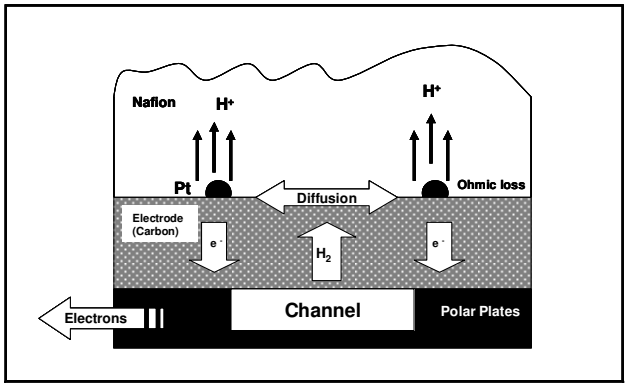

Figure 2. Transport and kinetic phenomena in the anodic compartment

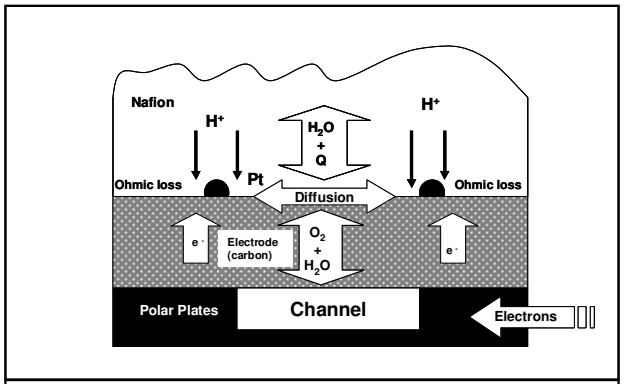

Figure 3. Transport and kinetic phenomena in the cathodic compartment

Nafion membrane as a perfluoro-sulfonated ionomer membrane is benchmark material in terms of performance, chemical and mechanical stability. These materials are generated by copolymerization of a perfluorinated vinyl ether co-monomer with tetrafluoroethylene (TFE). Although numerous studies are performed on alternative membranes, blends and composites, all results are systematically compared to Nafion membranes. However the Nafion structural models are mainly based on the Eisenberg description which considers ionic cluster dispersed in a hydrophobic polymeric matrix. Several molecular models have been published later [21, 22]: Yeager, Seko, Pineri, Perusich, Hashimoto, Gierke, Fujimura, Litt Dreyfus, Haubold and Rubatat. The source of debate on the morphology of Nafion stems from the fact that this ionomer has a unique chemical structure random, being capable of organizing a complex structure by ionic and crystalline regions. In these conditions Nafion structure may have a significant distribution size with a wide range of length scales [21]. The Yeager's model propose three regions in its structural chain for Nafion membrane (Figure 4): The first of these regions is a structure that contains chains of poly-tetrafluoetileno (PTFE), inert material in any environment or oxidation reduction with a characteristic hydrophobic and large chemical and mechanical stability. The second region named 'intermediary' is amorphous and hydrophobic, this contains chains hanging, a minimum quantity of water and some radical anions; The third region constitutes briquettes, ionic coexists where most ions sulphonated, cations and water molecules absorbed, giving a absorbing character to the membrane [23]. The sulfate ion present in the structure of Nafion allows the conductive properties in the terms of hydrated membrane, being an active site where some cations as H^+, Li^+, Na^+ among others, spreading by electro-absorption (pottering) into the membrane [22-29]. The particular molecule of water can also spread per share of bipolarity electrical by the hydrogen bridge. In a subsequent document Rubatat [31] and co. applied a combination of SAX and neutron scattering techniques including USAXS to characterize the state in Nafion hydrated within an interval of 1 to 1000 nm. Based on the results obtained, it's considered to be fundamentally characterized by the presence of elongated aggregates within the morphology of Nafion. The authors propose that the intermediate values in the intervals provide information related to the size, shape and spatial distribution of aggregates, while the very small can be attributed to packages largest aggregates (Figure 5) with a broad range of heterogeneous distribution. In 2000, Gebel proposed a structural

model for the membrane dry, whereas the ionic groups are isolated in an area with a diameter spherical and a distance of center to center and approximately 1.5 nm 2.7 nm, respectively. The water absorption allows kernels lengthening forming pools of water surrounded by groups in an ionic polymer-water interface in order to minimize energy interface. When increased water content in the membrane, it seems to "dissolve" in a solution, then the structures are separated to get a colloidal dispersion of isolated bars [32]. On the other hand, membrane drawings experiments have confirmed the “cylinder” model and the structure orientation effect on the protonic conductivity have been measured.

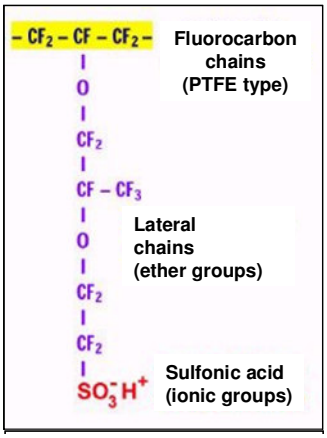

Figure 4. Nafion’s structure

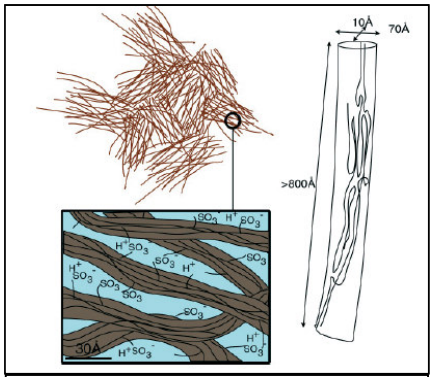

Figure 5. Schematic representation of an entangled network of elongated rodlike aggregates in Nafion [30].

This study proposes a statistical study by surface response methodology (SRM) for the electrical resistance measurements on the Nafion membranes surfaces, in order to know the surface characteristics for this property. The results may be important for suppose the possible effects on the PEMFC functionality by SER characteristics. The measurements are done on a Nafion 115 membrane (N115) without activation process (dehydrated) and other membrane at same type and lot previously

activated. The SRM is a mathematical and statistical collection tools useful in modeling and analysis of experimental problems, where the response (parameter interest) receive the influence of several variables [33], as follows:

$$y = f(x_1, x_2) + \varepsilon \quad \ldots\ldots (1)$$

where: X_1 and X_2 are the variables under review that affect the response; ε represents noise or error observed and y is the response. If the answer is denoted by:

$$E(y) = f(x_1, x_2) = \eta \ldots\ldots (2)$$

being E(y) the expected value and η is called as "surface response". In most applications the response surface area is represented by polynomials, those are used on the study region involved by the independent variables. The contours lines are drawn on the graphics to represent levels of response surface included constant values for X_1 and X_2, so to encourage the display of response surface form. Thus, the SRM is applied to find suitable approaches between a function and all independent variables, applying in first time a first order model as follow:

$$y = \beta_0 + \beta_1 x_1 + \beta_2 x_2 + \ldots + \beta_k x_k + \varepsilon \ldots\ldots (3)$$

When bends are observed in the system, it is hoped the implementation of a second-order model as described below:

$$y = \beta_0 + \sum_{i=1}^{k} \beta_i x_i + \sum \beta_{ii} x_i^2 + \sum_{i<j} \sum \beta_{ij} x_i x_j + \varepsilon \ldots\ldots (4)$$

The model describes a two-dimensional plane represented by the independent variables (X_i, X_j), being β the regression coefficients, and being y the expected value for the parameters electrical resistance on the flat two-dimensional surface.

2. EXPERIMENTAL PART

Two pieces of same lot of membrane N115 with an area defined in both cases at 112.33 cm^2 (10.5 x 10.7 cm), have been used in this study, one of them has been activated in the following manner: a dip in a 3% Vol, H_2O_2 solution at 80°C for an hour, then the membrane is immersed in deionized water to 80 ° C for one hour, after receiving a bath at the same temperature for two hours in a HNO_3 - 1 N solution, finally apply three bathrooms in deionized water [18]. Both membranes were geometrically divided into 4 quadrants with equivalent area to 5 x 5 cm for SER measurement. An experimental design 2^3 type central compound has been applied for measuring and recording of SER on the membrane N115. The measuring methodology has been detailed in first part of this study The equipment used for measurements of SER was a multimeter BK PRECISION model TEST BENCH®

390A. The statistical analysis was carried out in both membranes (activated and not) and on both sides of the same (A and B). The surface response analysis was obtained using the software Minitab V.15.

3. RESULTS AND DISCUSSION

Figure 6 shows the N115 membranes used in this study. Activated membrane (Figure 6.b) has increased his volume in 20.5 % during activation process. Water absorption and activation process has produced a modification in Nafion morphology in accordance with the literature [24, 31, 32]. Organic material and Nafion residuals may be the cause in brown coloration in not activated membrane (Figure 6.a). This material are removed and degraded by oxidation process with H_2O_2 during the first step at the activation process.

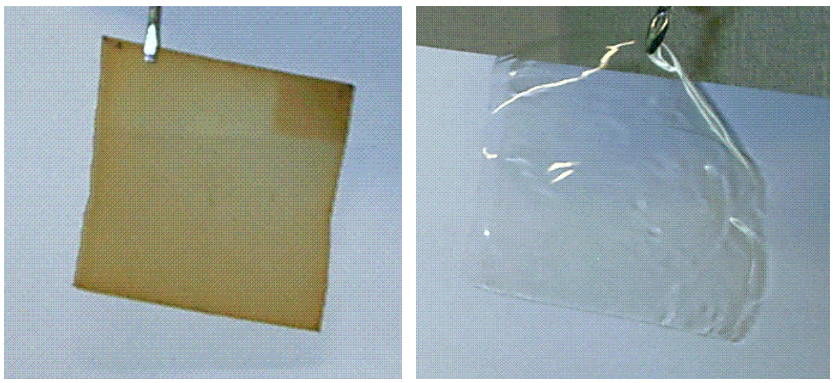

a) ***b)***

Figure 6. Nafion 115 membranes; a) not activated and b) activated

3.1. Not Activated Membrane

Applying the surface response methodology by using MINITAB software, were obtained the contour lines graphs showing the surface levels for SER on N115 membrane. Figure 7 shows the contour graphs for the SER measures recorded for not activated N115 membrane on side A for the four quadrants in which the membrane was geometrically sectioned. Overall figure shows a heterogeneous surface for the variable response (electrical resistance) in all quadrants, expressed by various curves and elevations in the level of graphics, therefore is possible to suppose that all surface in not activated N115 membrane is heterogeneous for electrical resistance property. Particularly, the first quadrant (Figure 7.a) introducing multiple levels of electrical resistance with bends closed on its surface characterization. Introducing a maximum toward the center left of its surface, while the second quadrant (Figure 7.b) is similar to that described above but at higher levels of resistance. In this quadrant, there is a maximum on the center right of its surface. The third quadrant (Figure 7.c) is also characterized by introducing multiple levels of electrical resistance with a greater number of bends, the maximum is observed right at the center of the figure, being a feature similar to the second quadrant.

Finally the fourth quadrant (Figure 7.d) is the only one who has a relative homogeneity in its central zone, showing elevations and depressions surface at the ends. Notable a valley with a common minimum value between III and IV quadrant, these contours are similar in shape but an orientation different is observed in comparison as Gierke's model for Nafion morphology [9], however, the overall contour graphs shows a random distribution of RES morphological areas similar to the model proposed by Rubatat and Coworkers [31].

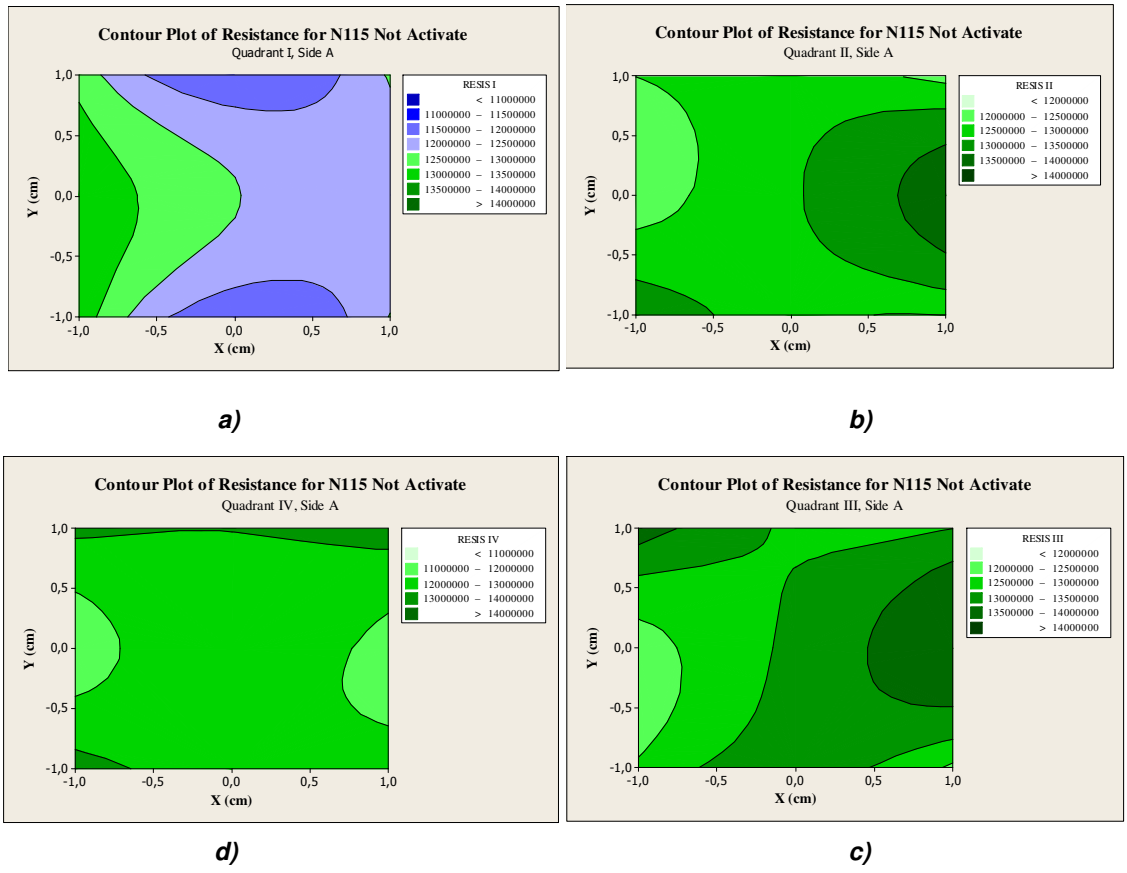

Figure 7. Contour graphics for SER for non activated N115 membrane at side A for; a) I, b) II, c) III and d) IV quadrants.

Figure 8 shows the 3D representations for the RES in all quadrants for not activated N115 membrane. It's observed in all 3D graphics some contortions and pronounced elevations. First quadrant (Figure 8.a) presents an irregular surface for RES with a plate zone at center right in the picture. Second quadrant is characterized by a minimum RES value at center left and a maximum value al center right in their picture, so a data correlation between both surfaces is possible if consider an space non registered inter pictures. Third quadrant (Figure 8.c) shows the biggest contoured area for SER property in the not activated membrane on side A and their elevations are higher. Similar to the second quadrant, a maximum value can be seen from the center right while a minimum value is present in the centre left in the picture, this part is possible to correlate with right side of fourth quadrant (Figure 8.d),

where value minimum for the SER is common to both images. The response surface in the fourth quadrant is relatively homogeneous compared to other cases.

Contour Graphics for the RES on the N115 dehydrated membrane on the side B are shown in Figure 9. In this graph set can be seen in greater curvature in elevation lines, there is also a greater randomness for SER zones in comparison with the side A. However there appears to be a match between the bottoms of the first quadrant with the top of the fourth quadrant where RES measurements are observed at levels at 12 MΩ. In other way, no maximum or minimum values are observed on the graphs because it's probably that SER measurements are taken around of this values but it's possible to observe the tendencies to maximum and minimum values.

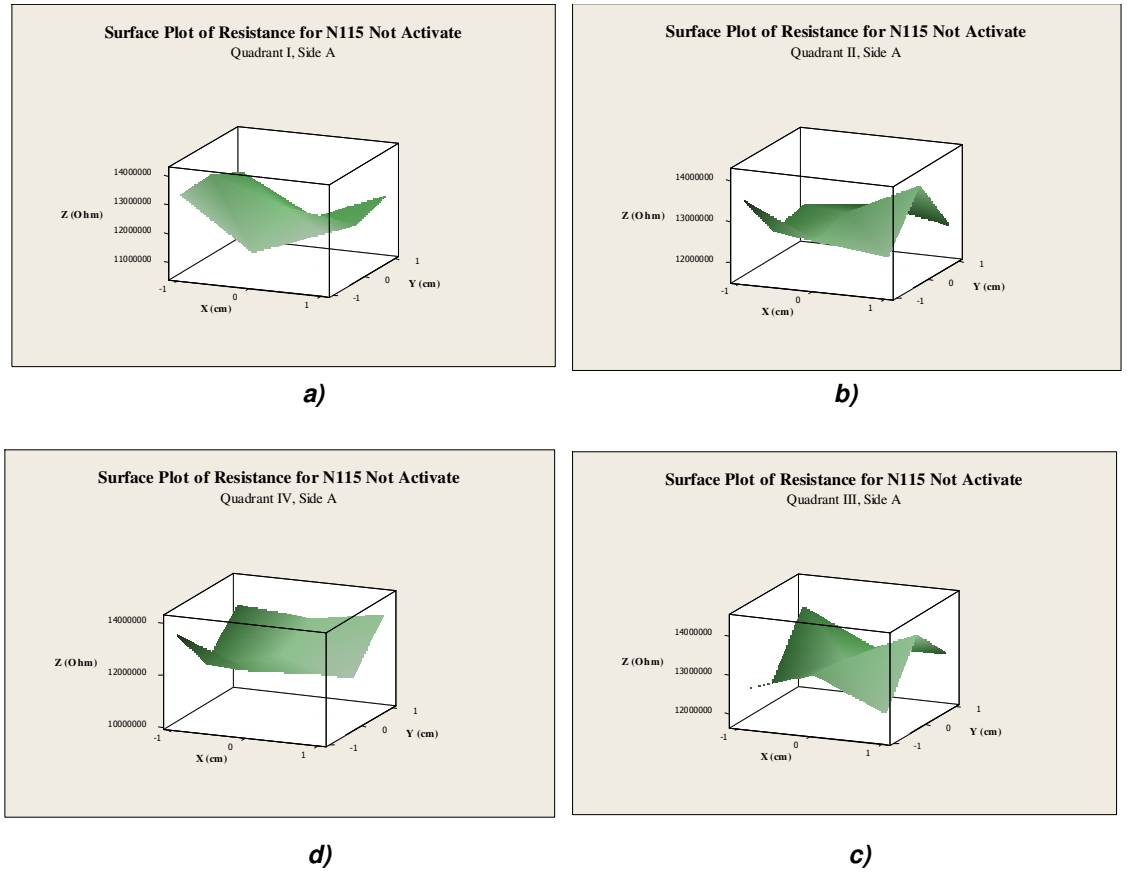

Figure 8. 3D Graphics for SER on not activated N115 membrane at side A for: a) I, b) II, c) III and d) IV quadrants.

In contour graphs for both sides (Figures 7 and 9) we can see that the quadrants II, III and IV presented to levels of around 1.2 E^{+7} Ohm (green) in addition to introducing similar morphologies. By contrast levels and morphology between the sides of the quadrant I look different to each others. Both sides have lower levels of RES represented in blue whereas in the other quadrants dominate higher levels represented in green colors.

Figure 10 shows the 3D graphics for the contour levels of RES for the second and fourth quadrant of the membrane N115 dehydrated on its side B. In the first quadrant (Figure 10.a) there is a considerable contortion with two surface elevations in opposite directions which suggests maximum values in these directions. In the second quadrant (Figure 10b) is a clear trend on the direction in which to place the highest value of RES in this region of the membrane, not seen evidence of any contour. Moreover, the picture shows the 10.c RES in the third quadrant of the membrane under consideration at its B side, in this area can see the various contortions displayed in the preceding sections, however the trend shows up to the bottom left of the figure. Finally Figure 10.d shows the trend RES fourth quadrant where there are pronounced contortions little except depression to the bottom left of the figure, a trend that suggests a minimum between the third and fourth quadrant B on the side of the membrane N115 unchecked.

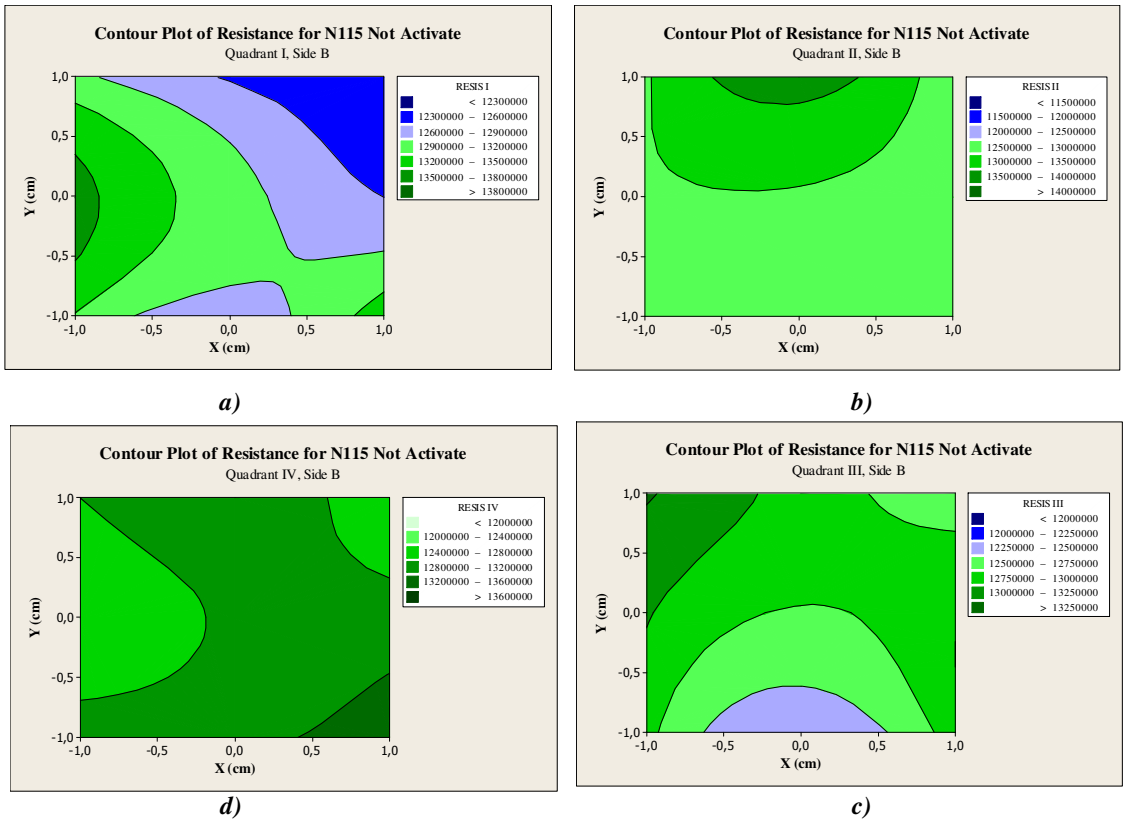

Figure 9. Contour graphics for SER on not activated N115 membrane at side B for; a) I, b) II, c) III and d) IV quadrants.

In principle a membrane without chemical activation has no application in the operation of the PEMFC. However these results are interesting surface represented by the characterization, being similar to the conditions RES when the membrane was dehydrated by the operation of the PEMFC at high temperatures or for long periods outside operation.

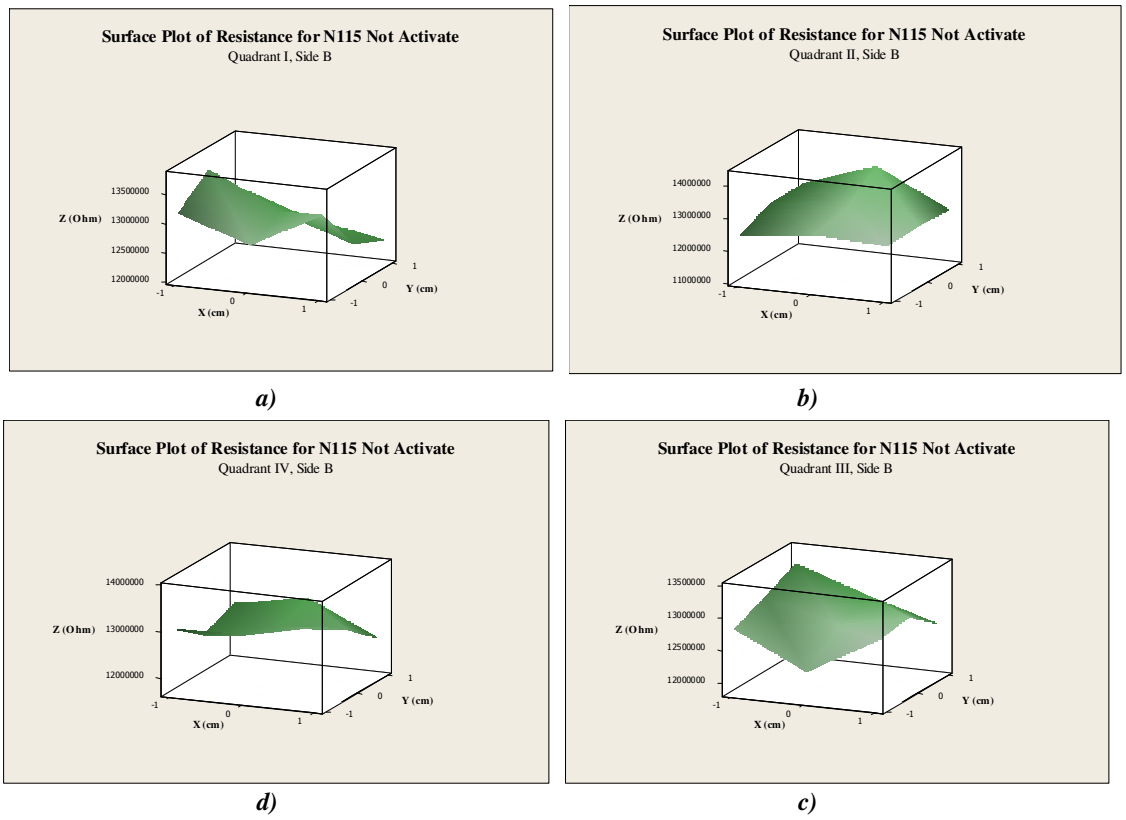

Figure 10. 3D Graphics for SER on not activated N115 membrane at side B for; a) I, b) II, c) III and d) IV quadrants.

3.2. Activated Membrane

In Figure 11 shows the contour graphs for RES recorded in the membrane N115 ® activated on side A for its four quadrants. In general there are heterogeneous levels for the variable in the study, levels show elevations and bends with the presence of maximum and minimum, moreover dominate overall levels in blue colors which represent lowest values for superficial electrical resistance in comparison with the green colors (highest), who are dominant in the not activated membrane. This indicates a significant reduction of SER on the activated membrane as a result the activation process chemistry. In the third quadrant is the only section of the membrane with a quasi-level heterogeneous (dark blue) for RES in the membrane N115, only a slight lift to the bottom left of the figure. Moreover, it is remarkable elevation in common between first and second quadrant (Figure 11.a and b), suggesting a maximum value present to the center between both pictures, this observation suggests an important correlation of experimental data. Even more surprising is observed on the two figures, the same as proposed by Gierke [9-10] for structural morphology in the Nafion membranes, in this case for the electrical resistance surface. A new case data correlation can be found at the bottom between the third and fourth quadrants of the membrane activated (Figure 11, c and d), where there is a common elevation, which also suggests the presence of a peak in that area. Therefore we can deduce the importance of molecular morphology on the electrical resistance characteristics in the Nafion

membrane. In PEMFC application, these maximum and minimum values in the SER must consequently affect the transport and kinetic phenomena during the fuel cell operation. It is hoped the presence of areas with the highest temperature (hot point) in the areas of greatest SER values when the PEMFC operating. Therefore an increase in the ohmic losses in the electrode-electrolyte interface is hoped with a decrease in the PEMFC efficiency. Even more, the more resistive side at the membrane in contact with the cathodic electrode submit more robust effects in loss efficiency.

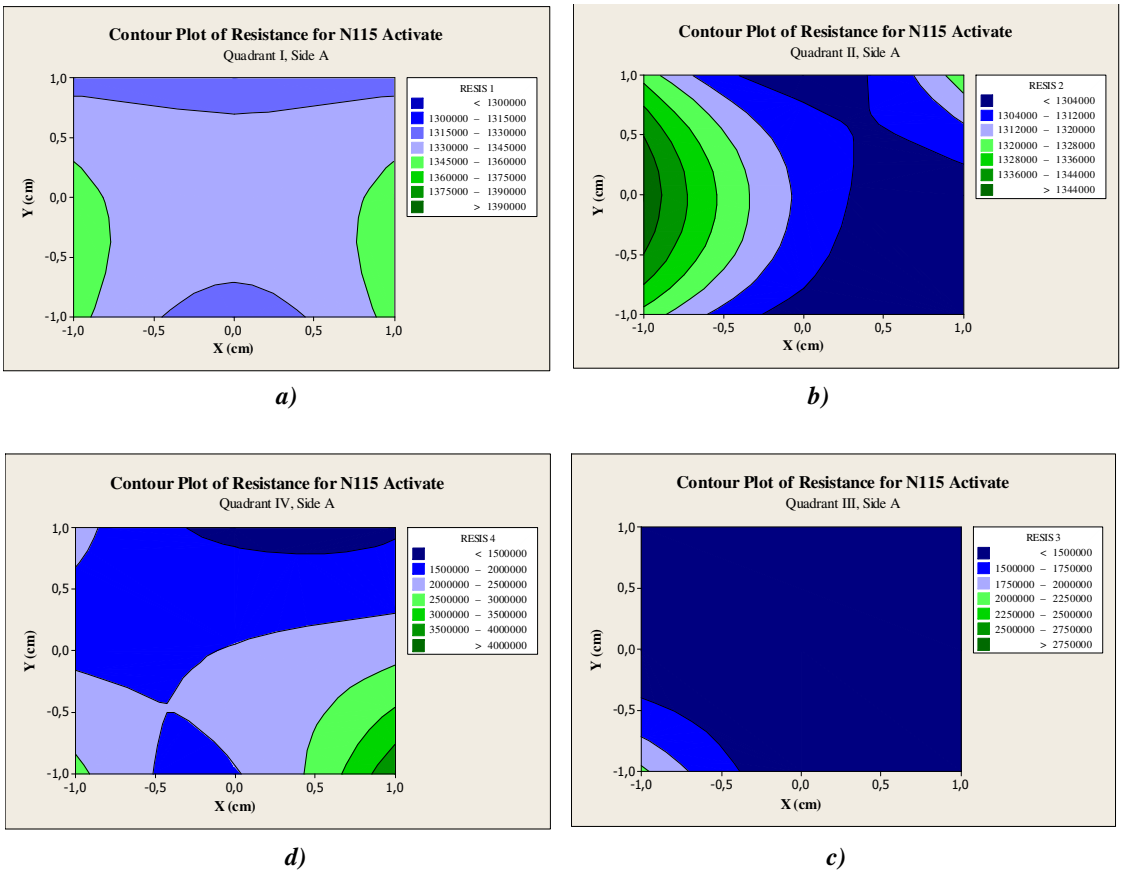

Figure 11. Contour graphics for SER on activated N115 membrane at side A for; a) I, b) II, c) III and d) IV quadrants.

Figure 12 shows the 3D graphics of the RES for the four quadrants of the membrane Nafion 115 activated on the side A. In the first quadrant (Figure 12.a) is observed a surface with a minimum value on a plate zone at center in the picture, sharp contours having the appearance of being relatively homogeneous in this zone, with features suited for a role in a cathodic PEMFC with minor ohmic losses. The second quadrant (Figure 12.b) is observed with elevations and contortions very pronounced, manifesting a rugged surface, unlike the previous section, this area is inappropriate for a cathodic activity in the PEMFC. The Figure 12.c shows an area cuasi-homogeneous except in the extreme left where there is a lower elevation, also has very low levels of electrical resistance (blue) to provide properties suitable for contact with the cathodic electrode in a PEMFC in operation. Finally

the surface SER at fourth quadrant is presented in Figure 12.d in which there is elevations and moderate depression, generating considerable contortions on the surface then this characteristics is inappropriate for a cathodic operation. In other way, a correlation is deduced between first and second quadrant, a maximum value (green color) is possible to exist into de both pictures. Others correlations are possible between bottoms in second quadrant with top at the third quadrant and this one with fourth quadrant at common zone between both images.

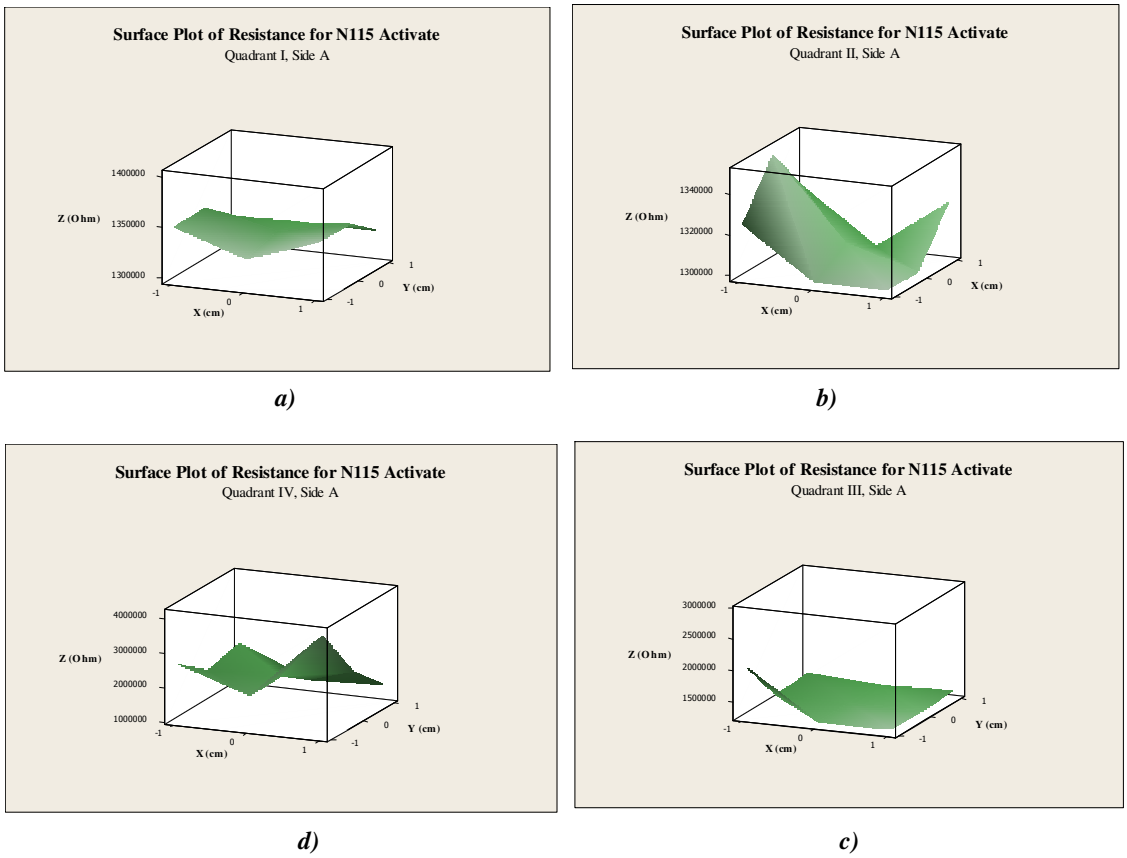

Figure 12. 3D Graphics for SER on activated N115 membrane at side A for; a) I, b) II, c) III and d) IV quadrants.

The graphics contour surface for SER in the membrane on the N115 on side B, are shown in Figure 13. It was generally observed heterogeneity in surface parameter studied, however unlike with side A for activated N115 membrane, in side B no correlations are observed between any quadrants but levels in green regions denote higher electrical resistance being even so, but their elevations are observed less pronounced. The surface for SER in the first quadrant (Figure 13.a) can be seen very homogeneous, introducing a slight depression in the center of the area; his blue color denotes a low electrical resistance. Notably, the side A (Figure 13.a) expressed the same characteristics; however, it's greater the uniformity in the side B. The Figure 13.b shows the SER response expected for the second quadrant at side B on activated N115 membrane, It's observed an homogeneous zone to half surface area at right on the picture, while at left side presents moderate elevations in the ends while the side A

(Figure 11.b) shows a very rugged surface. The SER surface for the third quadrant side B (Figure 13.c) shows some elevations and depressions on the surface mainly at the ends for which defines high contortions at right to the graph. Finally the SER surface for the fourth quadrant side B on activated N115 membrane is showed in Figure 13.d, it's observed a homogeneous zone with low electrical resistance and moderate elevations at the corners surface, considering at the center the electrode location, It's possible to consider this zone for a contact with the cathodic electrode in a PEMFC.

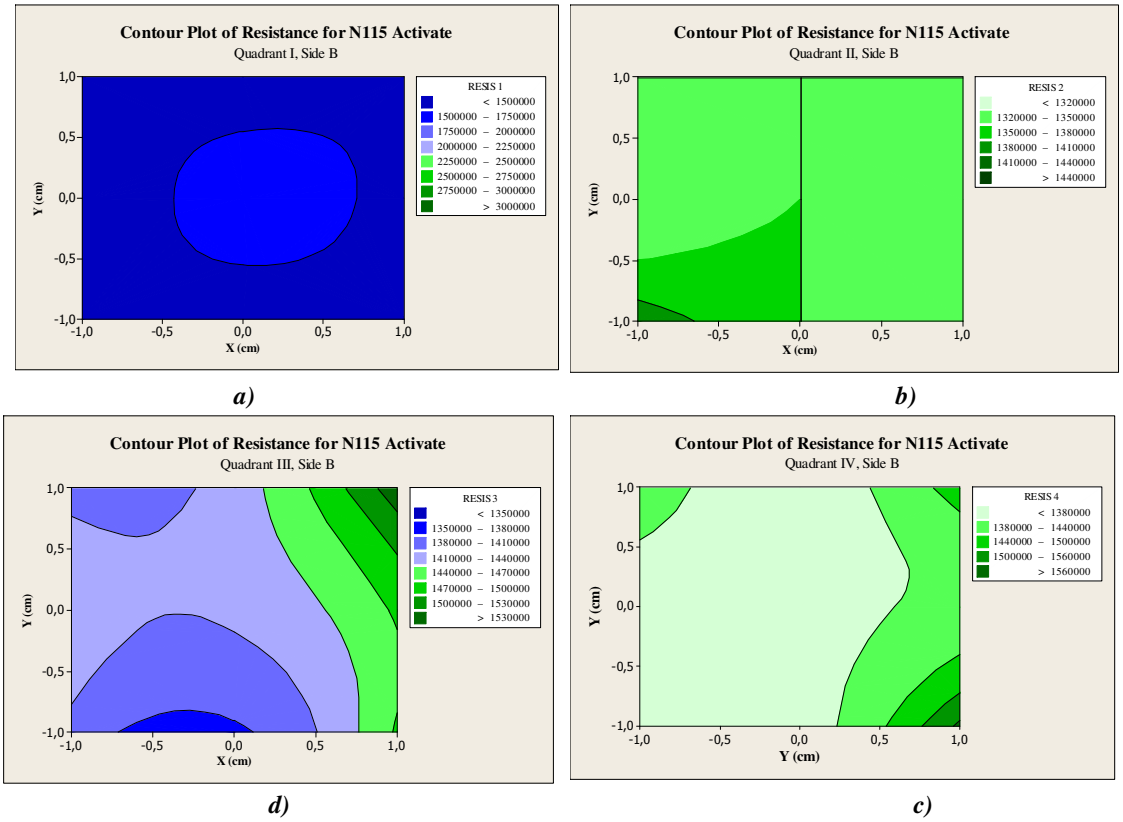

Figure 13. Contour graphics for SER on activated N115 membrane at side B for; a) I, b) II, c) III and d) IV quadrants.

The 3D graphics for variable-awaited response for side B side at activated N115 membrane is shown in Figure 14. The first quadrant (Figure 14.a) is characterized by a homogeneity particularly to low values of electrical resistance, this surface (side B)is more homogeneous and less resistive compared to the side A (Figure 12.a), so it is appropriate to his contact with the cathodic electrode during operation of a PEMFC. A similar SER surface can be seen for side B on 3D graph for second quadrant (Figure 14.b) where elevations are light in the corners on the left side, when compared with elevations of the A side, the side B is a more appropriate for cathodic operation in the fuel cell. In contrast, the prominence in surface elevation levels at the right on the 3D graph (Figure 14.c) for third quadrant of activated N115 membrane in comparison with the remarkable uniformity of the side A (Figure 12.c), advocating a better functioning of the PEMFC contacting the side B in discussion with

electrode anode. Finally, the SER surface for fourth quadrant presents moderate elevations in the corners at the graph in Figure14.d, as a behavior similar to same quadrant in side A (Figure 12.d), in contrast surface side B shows a valley with lower values in electrical resistance but their elevations are More high, therefore, when considering the location of the center electrode surface, the side B is desirable to cathodic compartment in a PEMFC operating.

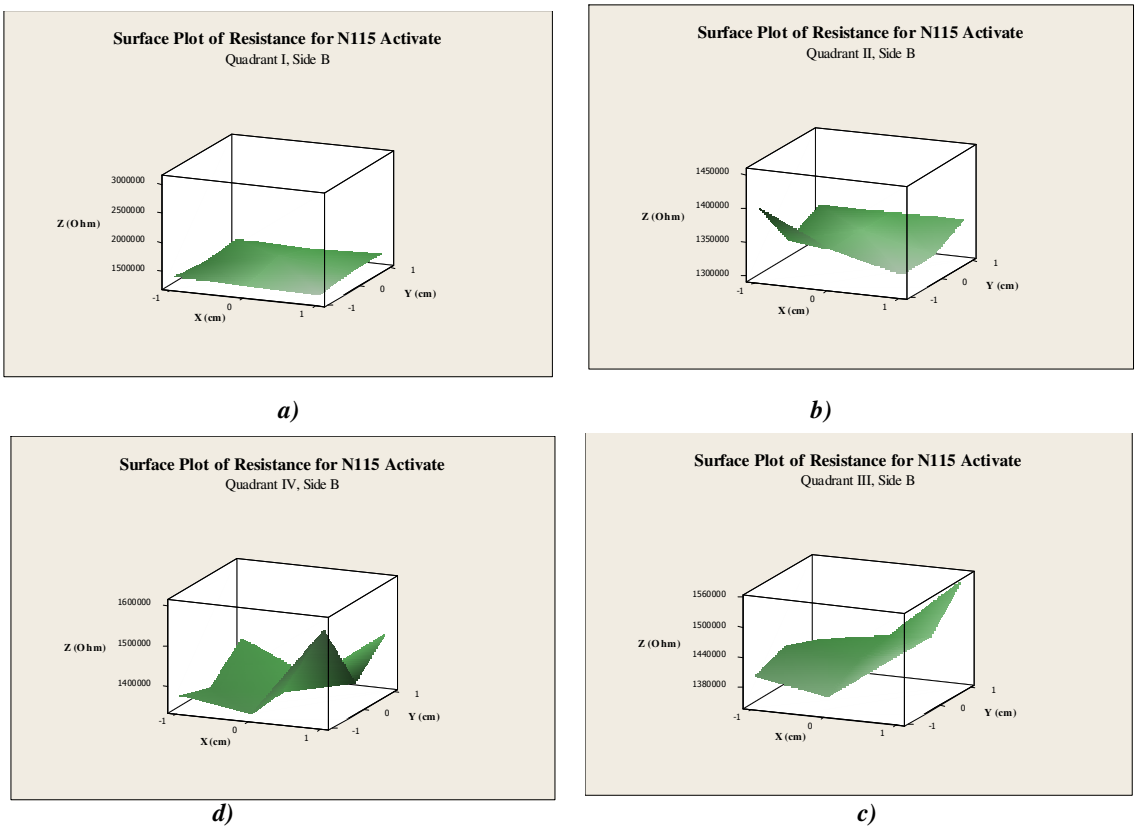

Figure 14. 3D Graphics for SER on activated N115 membrane at side A for; a) I, b) II, c) III and d) IV quadrants.

4. CONCLUSIONS

The results obtained by analyzing response surface show a general lack of standardization of electrical resistance on the surface of the Nafion 115 membrane for both treatments (activated and not). There is evidence at 95% in statistical reliability that superficial changes occur during chemical treatment process on the Nafion 115 membrane. The graphics contour surface for SER presents a similar forms to the structural morphology model proposed by Gierke and colleagues [24] for Nafion membrane. Moreover, the 3D and contour graphics for electrical resistance on surface of Nafion 115 membrane show the existence of random regions with different levels of electrical resistance, by its forms attributable to structural morphology proposal on the model of Rubatat [31] and redesigned by Gebel [32]. The reduction in electrical resistance values on Nafion 115 membrane is notable after

going through the activation process. There are significant differences in the level of RES between the sides of the N115 suggesting adverse effects on the functionality of a PEMFC according to contact with the cathodic electrode. Moreover the presence in SER with maximum and minimum zones on Nafion membrane suggests the presence of areas with the highest temperature (hot spots) during PEMFC operating.

References

1. V. S. Bagotzky, N. V. Osetrova and A. M. Skundin. *Russian Journal of Electrochemistry* 39 (2003) 919
2. P. Costamagna, S. Srinivasan. *Journal of Power Sources* 102 (2001) 242
3. P. Costamagna, S. Srinivasan. *Journal of Power Sources* 102(2001) 253
4. P. Costamagna. *Chemical engineering science* 56 (2001) 323
5. J.J. Bezian, *« Systèmes de piles a combustible pour la cogénération »,* Rapport de l'ADEME, Ecole des Mines de Paris, 1998
6. Electricité de France – Gas de France*, « Produire a la fois chaleur et électricité, c'est possible, avec la pile a combustible »*, Document issu du dossier de presse réalisé par EDF-GDF pour l'inauguration de la pile à combustible de Chelles (Seine-et-Marne), le 23/03/2000.
7. A. Heinzel, R. Nolte, K. Ledjeff-Hey and Zedda M. *Electrochimica Acta* 3 (1998) 3817
8. B. Emonts, J. Bogild Hansen, H. Schmidt, T. Grube, B. Höhlein, R. Peters, A. Tschauder. *Journal of Power Sources* 86 (2000) 228.
9. V. A. Paganin, E. A. Ticianelli, E. R. Gonzalez. *Journal of Power Sources* 70 (1998) 55
10. T. Susai, A. Kawakami, A. Hamada, Y. Miyake, Y. Azegami. *Journal of Power Sources* 92 (2001) 131
11. J. H. Lee, T. R. Lalk, A. J. Appleby. *Journal of power sources* 70 (1998) 258
12. D. L. Wood. III, S. Y. Jung and T. V. Nguyen. *Electrochimica Acta* 43 (1998) 3795
13. F. R. Kalhammer. *Solid State Ionics* 135 (2000) 315
14. C. Moisés Bautista-Rodríguez, Araceli Rosas-Paleta, Andrés Rodríguez-Castellanos, J. Antonio Rivera-Márquez, Omar Solorza-Feria, J. Antonio Guevara-Garcia, J. Ignacio Castillo-Velázquez., *Int. J. Electrochem. Sci.,* 2 (2007) 820
15. A. V. Anantaraman, G. L. Gardner. *J. Electroanal. Chem* 414(1996) 115
16. C. K. Nguy. « Elaboration des membranes composites alternatives au Nafion pour piles à combustible H2-O2», DEA de l'INPG (1996)
17. K. B. PRATER. *J. Power Sources* 51(1994) 129
18. G. A. Pourcelli, A. Oikonomen, C. Gavach and H. D. Hurwitz. *J. Electroanal. Chem*. 259 (1989) 113
19. B. Tazi, O. Savadogo. *Electrochimica Acta* 45 (2000) 4329.
20. J. J. Fontanella, M. C. Wintersgill, R. S. Chen, Y. Wu and S. G. Greenbaum. *Electrochimica Acta* 40 (1995) 2321
21. K. A. Mauritz, R. B. Moore. *Chemical Reviews* 104 (2004) 4535
22. R. Mosdale. « Etude et développement d'une pile à combustible hydrogène/oxygène en technologie électrolyte polymère solide », Thèse Doctorale de l'INPG 1992.
23. H. L. Yeager and A. Steck. *J. Electrochem. Soc.* 128 (1981) 1880
24. T. D. Gierke, G. E. Munn, F. C. Wilson. *J. Polymer Sci., Polymer Phys* 19 (1981) 1687
25. W. Y. Hsu, T. D. Gierke. *Macromolecules* 15 (1982) 101
26. W. Y. Hsu, T. D. Gierke. *J. Membrane Sci*. 13 (1983) 307
27. R. A. Register and S. L. Cooper. *Macromolecules* 25 (1990) 318
28. G. Xu. *Polymer* 25 (1993) 397

29. T. Xue, Y. S. Trent and K. Osseo-Asare. *J. Membrane Sci.* 45 (1989) 261
30. S. Rieberger and K. H. Norian. *Ultramicroscopy* 41 (1992) 225
31. L. Rubatat, A-L. Rollet, G. Gebel, O. Diat *Macromolecules* 35 (2002) 4050
32. G. Gebel. *Polymer* 41 (2000) 5829
33. D. C. Montgomery and G. C. Runder. "Design and Analysis of Experiments", 2nd version, Ed. Limusa & Wiley, 2007, USA.